Heliyon 6 (2020) e04763

Contents lists available at ScienceDirect

Heliyon

journal homepage: www.cell.com/heliyon

Research article

Chemical, structural, and thermal characterization of starches from four yellow Arracacha (*Arracacia xanthorriza*) roots produced in Colombia

Magda I. Pinzon [a,**], Leidy T. Sanchez [a], Cristian C. Villa [b,*]

[a] Programa de Ingenieria de Alimentos, Facultad de Ciencias Agroindustriales, Universidad del Quindio, Carrera 15 Calle 12N, Armenia, Quindío, Colombia
[b] Programa de Quimica, Facultad de Ciencias Basicas y Tecnologias, Universidad del Quindio, Carrera 15 Calle 12N, Armenia, Quindío, Colombia

ARTICLE INFO

Keywords:
Food science
Food analysis
Arracacha
Peruvian carrot starch
Andean tubers

ABSTRACT

In recent years, interest has increased in the search for new starch sources, especially among Andean tubers, such as Arracacha (or Peruvian Carrot). This work studied the chemical composition, structural features, and thermal and adsorption properties of four sub-varieties of yellow Arracacha grown in Colombia: comun (Com), cartagenera (Car), yema de huevo (YH) and clon 22 (C22). Starches from the Com, Car and YH sub varieties presented similar properties, amylose content around 30%, relative crystallinity around 31% and gelatinization temperature around 60 °C. On the other hand, starch from the *Clon 22* (*C22*) variety presented the highest amylose content, leading to an increase in gelatinization temperature (63 °C), and lower relative crystallinity (24%). Furthermore, digestibility studies show that C22 presented a higher resistant starch content. Our results show that Arracacha is a very interesting starch source, despite few studies on the properties of the different sub-varieties.

1. Introduction

Arracacha or Peruvian carrot (*Arracacia xanthorriza*) is a native tuber of the Andean region in South America in countries, like Colombia, Peru, Bolivia, and Ecuador (Castanha et al., 2018; Londoño-Restrepo et al., 2018; Lovera et al., 2017). Traditionally, Arracacha ranks among the main carbohydrate sources in said countries, alongside potatoes, plantains, and cassava due to its traditional use in culinary dishes(dos Santos et al., 2018; Gutiérrez Malaxechebarría, 2011; Moraes et al., 2014; Rocha et al., 2011). In recent years, interest in Arracacha has increased, especially in Colombia where crops have grown considerably, however, it is still and underused product, that could have many applications in different areas of the food industry (Gutiérrez Malaxechebarría, 2011). Likewise, there is a growing interest i in the food industry for new starch sources, such as Andean tubers, which can be used as food ingredients and additives (Castanha et al., 2018; Cisneros et al., 2009; Cruz et al., 2016).

Starch is produced by most plants as an energy reserve, being the second most-common biomass on earth after celluloses (Wang et al., 2015). It is found as small granules of different morphologies in plant tissues, mainly seed, roots, tubers, leaves, and fruits (Magallanes-Cruz et al., 2017; Tappiban et al., 2019; Villa et al., 2019; Wang et al., 2015). The chemical structure of starch is classified as a polysaccharide composed of α-D-glucopyranosyl units that can be linked in either α-D-(1–4) and/or α-D-(1–6) linkages (Magallanes-Cruz et al., 2017). Due to these two types of linkages, two molecules can be found in the starch granules: the linear amylose formed by glucose units linked in α-D-(1–4) manner and the branched amylopectin, formed by glucose units branched through α-D-(1–6) linkages (Magallanes-Cruz et al., 2017). The amylose/amylopectin ratio in the starch granule is heavily dependent on the botanical sources and cultivar conditions. Common native starches have amylose percentages that range between 20% and 30% and amylopectin ranging from 70% to 80%. Likewise, there are starch granules with higher amylopectin content, such as waxy maize and waxy rice starch.

One of the main characteristics of Arracacha is that it can be classified into three main varieties, easily identifiable by their pulp color: white, yellow and purple with many sub-varieties from each color. Recently, studies have focused on characterizing starches from those three Arracacha varieties, reporting small differences among them, especially in their thermal properties (Castanha et al., 2018; Londoño-Restrepo et al., 2018). Furthermore, the authors reported that Arracacha starches tend to have low gelatinization temperature and high water absorption capacity. There are many sub-varieties related to each of the main color varieties.

* Corresponding author.
** Corresponding author.
E-mail addresses: mipinzon@uniquindio.edu.co (M.I. Pinzon), ccvilla@uniquindio.edu.co (C.C. Villa).

https://doi.org/10.1016/j.heliyon.2020.e04763
Received 27 May 2020; Received in revised form 19 June 2020; Accepted 18 August 2020

They usually differ in the physical appearance of the tuber, and some traditional gastronomic uses, however, to the best of our knowledge, no studies exist on the characterization properties of starches from the different Arracacha sub-varieties of the same pulp color. Therefore, this work studied the structural characteristics, such as granule morphology, particle size, relative crystallinity and branching degree of starches from four sub-varieties of yellow Arracacha grown in Colombia. Results from thermal properties, such as gelatinization and pasting properties are also reported, in order to increase the possible applications of this important Andean tuber in the food industry.

2. Materials and methods

2.1. Materials

Arracacha tubers from four yellow sub-varieties: *Comun* (Com); *Cartagenera* (Car); *Clon-22* (C22), and *Yema de Huevo* (YH) were kindly provided by AGROSAVIA from their experimental cultivar in Cajamarca (Tolima), Colombia. Roots were harvested in April 2018 and rapidly transported to the Postharvest Research Laboratory in Armenia (Quindío), Colombia for starch isolation and further analysis.

2.2. Starch isolation

Starch isolation was carried out according to the method described by Acevedo-Guevara et al. (2018) with some modifications. In brief, Arracacha tubers were carefully washed and peeled with a kitchen knife. Then, they were cut into 2-cm slices and blended for 2 min. The homogenate was then washed through screens (20, 40, and 60 US mesh) to eliminate fiber residues; thereafter, the solution was left to decant during 3 h. The white starch sediments were dried in a Digitronic J.P Selecta hot-air oven at 40 °C during 48 h. The solids were ground with a pestle and passed through a sieve (100 US mesh) and placed into a sealed container and stored at room temperature until required.

2.3. Compositional characterization

Compositional analysis of the isolated starches was carried out by using the following methods: dry matter via the 934.06 AOAC method (AOAC; 1990); protein analysis was performed by using the 960.52 method (AOAC, 2002); fat content was determined by using the 960.39 method (AOAC, 2002); and crude ash content was determined by using the 923.03 method (AOAC, 2002). Total starch content was determined using an enzymatic starch determination kit (Megazyme International, Wicklow, Ireland) as reported by Chávez-Salazar et al. (2017) Finally, amylose content was determined through the colorimetric method proposed by Ambardekar et al. (2011).

2.4. Structural characterization

2.4.1. Morphology and particle size

Granule morphology and particle size were studied by using Scanning Electron Microscopy (SEM). Analyses were carried out in a FEI QUANTA 250 SEM microscope (Oberkochen, Germany). Samples were placed on circular aluminum stubs with double-sided carbon adhesive tape and images were captured at different magnifications. Mean particle size was determined from the SEM images by using the ImageJ software (ver. 1.49, National Institutes of Health, USA). Mean particle for each sub variety was calculated by measuring 100 starch granules, from different micrographs of the same sample. Furthermore, three different starch samples from each sub variety were used.

Polarized Light Microscopy (PLM) analyses were carried out on a polarized microscope (BX41, Olympus, Japan). A droplet of the starch slurry was applied to microscopic observation and images were taken at different magnifications.

2.4.2. X-ray diffraction

X-ray diffraction (XRD) patterns were obtained in a Bruker D8 Advance X-ray diffractometer operated at 40 kV and 100 mA with a Cu–K, radiation ($\lambda = 1.54$ Å). All samples were scanned through the 2θ range from 5 – 40°, with a continuous scan mode at room temperature. Relative crystallinity was calculated as the ratio of the crystalline area to the total diffraction pattern area, as reported by Zeng et al. (2016) using Eq. (1):

$$Relative\ Crystallinity\ (\%RC) = \frac{A_c}{A_c + A_a} x\ 100 \quad (1)$$

where A_c is the area of the crystalline region and A_a is the area of the amorphous region of the diffraction pattern.

2.4.3. FTIR

In order to understand the structure of the four yellow Arracacha starches studied, several techniques were used; among those techniques, Fourier transform infrared (FTIR) can be used to understand several aspects of the starch granule composition and internal structure as it based in the vibrations of chemical bonds due to infrared radiation (Dankar et al., 2018; Sevenou et al., 2002). FTIR analyses were performed by using a Prestige 21 Shimadzu FTIR spectrophotometer. All the samples were pressed as pellets with potassium bromide (KBr), dried, and placed in the FTIR spectrophotometer. Transmittances were recorded at wave numbers between 4000 and 400 cm^{-1} at a resolution of 2 cm^{-1}.

2.4.4. ^1H NMR

^1H NMR spectroscopy studies were performed as reported by Schmitz et al. (2009) and modified by Tizzotti et al. (2011). In brief, approximately 10 mg of starch were mixed with 1 mL of anhydrous DMSO- d_6 in glass vials. The mixture was gently stirred and the vials were sealed with Parafilm. The vials were then homogenized in a shaking bath at 70 °C and 300 rpm during 48 h; 28 μL of TFA-d_1 were added to the samples just before NMR measurement, and the mixture was transferred to 5 mm NMR tubes. Analyses were carried out in Bruker spectrometer operating at a frequency of 400 MHz for ^1H. Spectra were recorded at 70 °C and analyzed by using the Bruker TopSpin version 4.0.7 software. All spectra were manually phased and baseline-corrected. A Lorentzian fit was used for spectral deconvolution.

Degree of branching (DB), expressed as the number of branching points with respect of the total number of glucosidic linkages, was calculated as reported by Tizzotti et al. (2011) by using Eq. (2):

$$DB\ (\%) = \frac{I_{\alpha-1,6}}{I_{\alpha-1,6} + I_{\alpha-1,4}} x\ 100 \quad (2)$$

where, $I_{\alpha\text{-}1,6}$ and $I_{\alpha\text{-}1,4}$ represent the ^1H NMR integrals of the signals of the anomeric carbons of the α-1,6 and α-1,4 linkages at 5.11 and 4.75 ppm, respectively.

2.5. Thermal properties

2.5.1. Gelatinization

Differential scanning calorimetry (DSC) studies were carried out in a DSC- 214 Polyma-Netzsch (Germany) equipment. Samples were dried at (50°) for 16 h to remove all moisture content. An appropriate amount of the samples (2–3 mg) were weighed in an aluminum pan and 6–7 μL of water was added. The pans were sealed and the samples were heated from 25 to 105 °C at a 5 °C/min rate; an empty pan was used as reference. Runs were operated under a N_2 atmosphere (30 mL/min). The DSC thermograms were analyzed, as well as T_0 (onset temperature), T_p (peak temperature), and ΔH_g (gelatinization enthalpy).

Table 1. Chemical composition of yellow Arracacha starches.

Starch	Starch (%)	Lipids (%)	Protein (%)	Ash (%)	Amylose (%)
Com	98.1 ± 0.3[a]	0.06 ± 0.02[a]	0.11% ± 0.05[a]	0.16 ± 0.08[a]	29.03 ± 0.18[a]
Car	97.2 ± 0.2[b]	0.05 ± 0.02[ab]	0.14% ± 0.08[a]	0.12 ± 0.04[a]	29.21 ± 0.64[a]
C22	98.4 ± 0.2[a]	0.03 ± 0.01[b]	0.12% ± 0.04[a]	0.10 ± 0.03[a]	34.31 ± 0.19[b]
YH	96.8 ± 0.8[b]	0.03 ± 0.01[b]	0.12% ± 0.05[a]	0.15 ± 0.04[a]	30.31 ± 0.13[a]

Means with different superscripts are significantly different in their respective column ($p < 0.05$).

2.5.2. RVA

Pasting profiles were obtained with a Rapid Visco Analyzer (RVA) model RVA-4 series (Newport Scientific, Warriewood, Australia). An appropriate amount of starch (dry base) was dispersed in distilled water in 25 mL of water to obtain 5% suspension. Analyses were performed by using the following temperature profile: samples were held at 50 °C for 1 min, then heated from 50 to 90 °C at a 6 °C/min rate. Temperature was held at 90 °C for 5 min, then cooled to 50 °C at a 6 °C/min rate under continuous stirring at 160 rpm. Pasting temperature (PT), peak viscosity (PV), hot paste viscosity (HPV) at the end of the temperature plateau at 90 °C, and the cool paste viscosity (CPV) at 50 °C, breakdown (BD), total setback (SB), and consistency (CS) were determined.

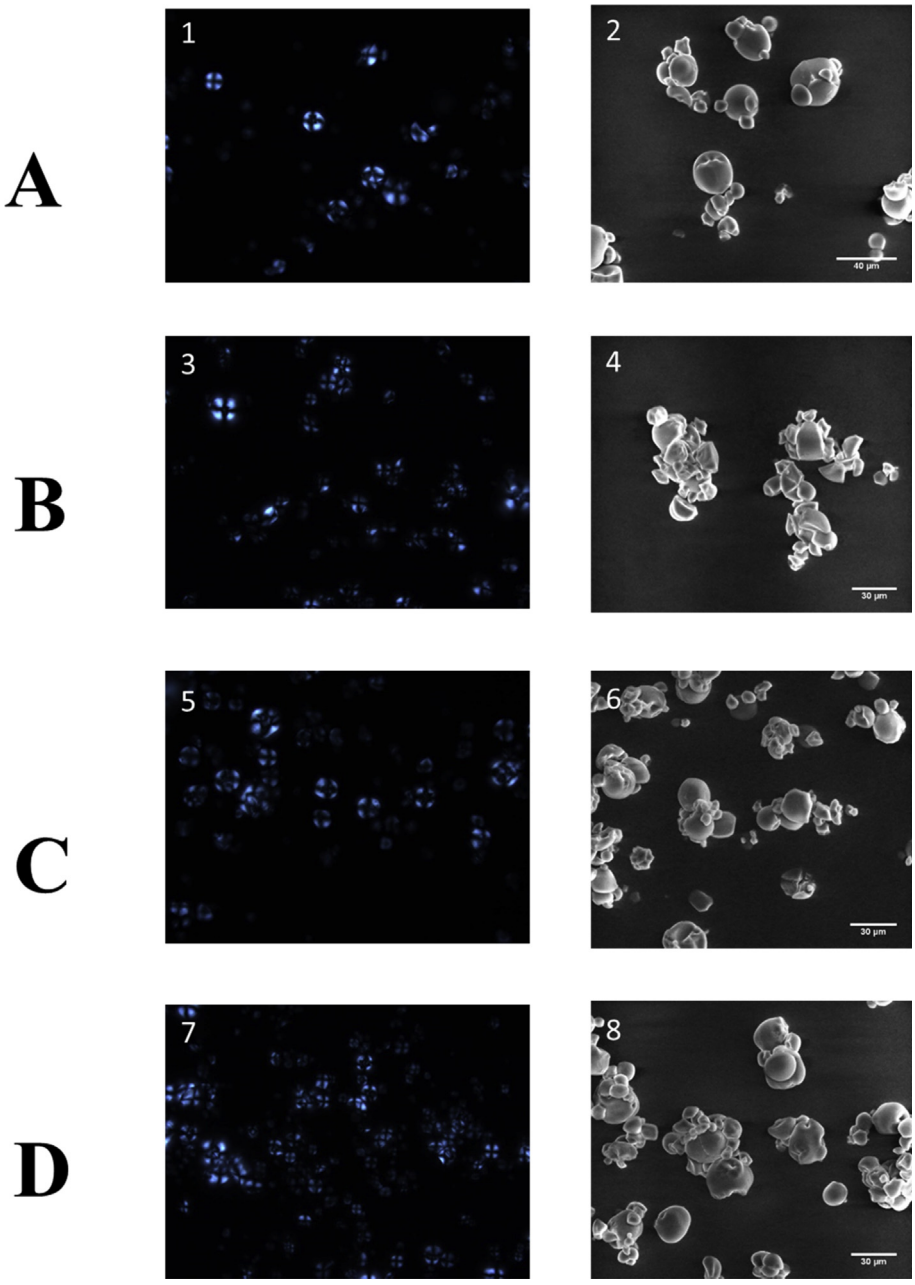

Figure 1. Polarized Light of the yellow Arracacha starches. A1) *Com*; B3) *Car*; C5) *C22;* D7) YH and Scanning Electron Microscopy images of the yellow Arracacha starches. A2) *Com*; B4) *Car*; C6) *C22;* D8) YH.

2.6. In-vitro starch digestion

The rapidly digestible starch (RDS), slowly digestible starch (SDS), and resistant starch (RS) fractions of the four Arracacha starches were determined according to Chung et al. (2009). In brief, 0.1 g of Arracacha starch were mixed with 4 ml of sodium acetate buffer (0.5 M, pH = 5.2). An enzymatic solution was prepared by mixing 2.7 mL of porcine pancreatic α-amylase (0.11 g/mL) and 0.3 mL of amyloglucosidase. The enzyme solution was freshly prepared for each digestion. The starch suspension was mixed with 1 mL of the enzymatic solution and incubated in a shaking water bath at 37 °C (200 rpm). Aliquots of 0.1 mL were taken every 20 min and hydrolyzed glucose content was measured by glucose oxidase-peroxidase reagent.

2.7. Water sorption isotherms

Water sorption isotherms were determined as proposed by Thys et al. (2010). Different salts ($CaCO_3$, NaCl, and KCl) and H_2SO_4 were used to produce relative humidity ranging from 10% to 98%. Arracacha starch samples were placed into a desiccator containing H_2SO_4 for over one month (until constant weight) to reach water contents of 3% (w.b) and ensure the adsorption process. Samples of about 2 g of Arracacha starch were placed in small plastic containers and then stored inside a sealed desiccator, with the different solutions for each different relative humidity (10; 33; 47; 75; 87; 98%). The desiccator was left in temperature controlled room (25 °C) until equilibrium was been reached. Samples were weighed every 7 days until constant weight was reached. The experimental data for the adsorption isotherms obtained was fitted to the B.E.T and G.A.B models.

2.8. Statistical analysis

All experiments were carried out in triplicate and results were analyzed by multifactor analysis of variance (ANOVA) with 95% significance level using Statgraphics® Plus 5.1. Multiple comparisons were performed through 95% least significant difference (LSD) intervals.

3. Results and discussion

3.1. Compositional analysis

The compositional analysis of the four yellow Arracacha starches is presented in Table 1. All four starches showed lipid, starch and ash content below 1%, with *Com* Arracacha starch showing the highest lipid value. These values agree with previous reports of the compositional content of Arracacha and other tuber starches (Castanha et al., 2018; Londoño-Restrepo et al., 2018; Yong et al., 2018; Zhang et al., 2018). Furthermore, all four Arracacha samples showed starch content above 95%, with the *Com* and *C22* varieties presenting values above 98%. Results agree with the report by Londoño-Restrepo et al. (2018) in which yellow Arracacha presented the highest starch content among the main colored Arracacha varieties. Finally, amylose content for *Com*, *Car*, and *YH* varieties did not present any significant difference among them, with values in the 31%–32% range. On the other hand, starch from the *C22* variety showed an amylose content of 34.31 ± 0.19%. Both, Londoño-Restrepo et al. (2018) and Castanha et al. (2018) reported amylose content above 30% for yellow Arracacha starch, however, Rocha et al. (2011) reported amylose content around 20% for the "*Amarela de Senador Amaral*" yellow Arracacha sub-variety. Those results indicate a wide range of amylose content among the sub-varieties of yellow Arracacha.

3.2. Morphology of the starch granules

Figure 1 presents the SEM and polarized light microscopy images for all four starches studied. The *Car* starch showed polyhedral morphology, while the other three starches presented more ovoid, almost spherical, morphology. Recently, Londoño-Restrepo et al. (2018) reported that starch from Arracacha roots produced in Colombia presented a mixture of round shaped and polyhedral morphologies. Furthermore, some of the

Table 2. Morphology, particle size, relative crystallinity (RC) and degree of branching (DB) of the different yellow Arracacha Starches.

Starch	Morphology	Mean Particle size (μm)	RC (%)	DB (%)
Com	Ovoid	9.81 ± 2.23[a]	31.54 ± 1.14[a]	3.38 ± 0.03[a]
Car	Polyhedral	10.11 ± 1.89[a]	31.43 ± 1.35[a]	3.33 ± 0.04[a]
C22	Ovoid	11.06 ± 2.15[a]	24.03 ± 1.12[b]	3.09 ± 0.02[b]
YH	Ovoid	13.74 ± 2.18[a]	31.48 ± 1.11[a]	3.38 ± 0.02[a]

Means with different superscripts are significantly different in their respective column ($p < 0.05$).

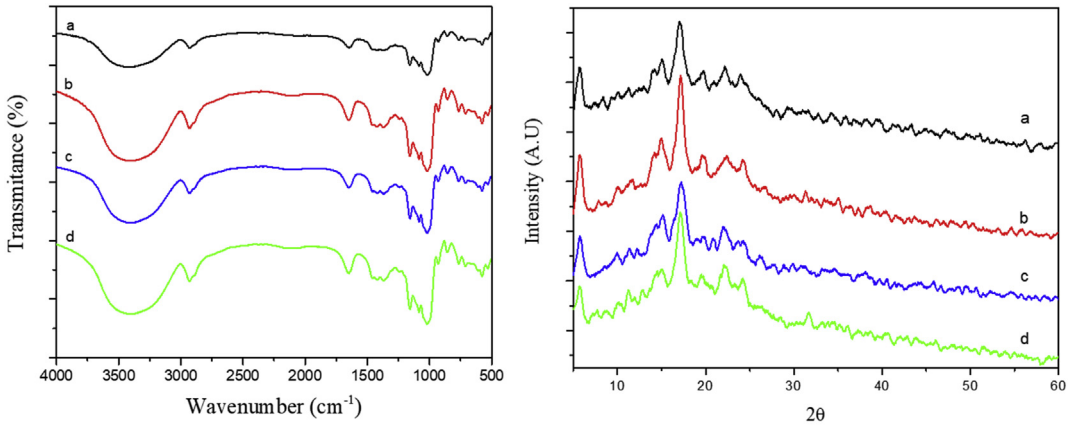

Figure 2. I) FTIR spectra and II) XRD diffractograms of the four yellow Arracacha starches. a) *Com;* b) *Car*; c) *C22*; *and* d) *YH*.

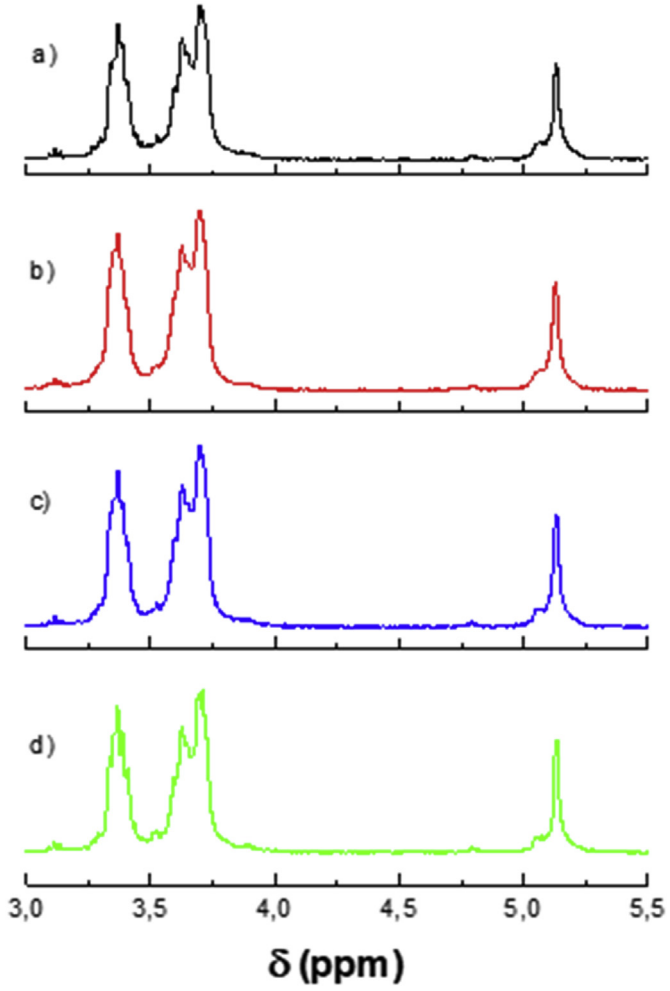

Figure 3. ^{1}H NMR spectra of the four yellow Arracacha starches. a) *Com;* b) *Car*; c) *C22*; and d) *YH*.

starch granules had surface cracks and fissures that can be attributed to the compressed Lego-like structure previously reported for Arracacha and Mafafa starches (Castanha et al., 2018; Londoño-Restrepo et al., 2014, 2018) Likewise, Figure 1 shows the PL micrographs of the different yellow Arracacha starches. All samples presented a well-defined birefringence pattern with a dark cross. Birefringence is a common feature of the starch granule structure and implies a high degree of molecular orientation within the granule. As for granule sizes, all four yellow Arracacha starches presented very similar values. As shown in Table 2, particle size ranged from 9.81 ± 2.23 to 13.74 ± 2.18 μm, with no significant difference among them.

3.3. Structural characterization

Figure 2-II shows the XRD patterns of the different Arracacha starches. All samples presented peaks at 2θ = 5.7°, 14.9°, 17.1°, 19.1°, 22.1°, and 24.2° that correspond to the semi-crystalline nature of the granule and the B-type structure commonly assigned to starches from Andean tubers (Cisneros et al., 2009; Cortella and Pochettino, 1995; Cruz et al., 2016; Vieira and Sarmento, 2008). The RC for the *Com*, *Car*, and *YH* starches was around 31%, as shown in Table 2, values that agree with previous studies reporting RC values for Arracacha starch above 30% (Moraes et al., 2013; Moraes et al., 2014; Rocha et al., 2011; Vieira and Sarmento, 2008). Although the diffraction patterns of the four yellow Arracacha starches showed no significant difference in their characteristic peaks, the RC of the *C22* starch differed significantly ($p < 0.05$) from

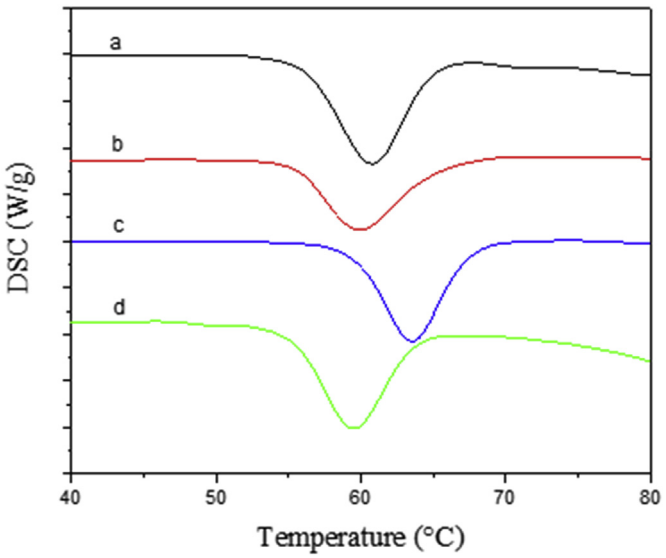

Figure 4. DSC thermograms of the four yellow Arracacha starches. a) *Com;* b) *Car*; c) *C22*; and d) *YH*.

the other three starch samples studied, with values around 24.03 ± 1.12 (Table 2). Previous studies have shown negative correlation between the amylose content and RC of the starch granules, given that the linear amylose molecules disrupt the crystalline packing of highly branched amylopectin molecules (Atichokudom-chai et al., 2001; Cai et al., 2015; Chung et al., 2011). Thus, because *C22* had a higher amylose content than the other three Arracacha starches, a lower RC value was expected.

Figure 2-I shows the FTIR spectra of all Arracacha starches. There was no significant difference among the four spectra, presenting the peaks and bands characteristic of the starch granule structure. The broad band in the 3700–3000 cm^{-1} region has been attributed to the stretching modes of OH groups, while the bands at 1157, 1105, and 982 cm^{-1} are commonly attributed to C–O and C–C stretching with some C–OH contributions (Pozo et al., 2018). Furthermore, the peaks at 1409 and 1433 cm^{-1} are associated with the C–H bending of CH_2 and the peaks at 1240, 1299, and 1333 cm^{-1} are associated with O–H bending (Pozo et al., 2018).

Finally, ^{1}H NMR spectra in the region from 3.0 to 5.5 ppm of all four Arracacha starches are shown in Figure 3. Degree of branching (DB) was calculated from the ^{1}H NMR spectra and as shown in Table 2. The DB results showed no significant difference among the *Com*, *Car*, and *YH* varieties, with values in the range from 3.33% to 3.38%, while starch from the *C22* variety had a DB of 3.09 ± 0.02% ($p < 0.05$). The DB is expressed as the percentage of α-(1–6) glycosidic linkages or branching points from the amylopectin molecules to the total of both α-(1–4) and α-(1–6) glycosidic linkages (Syahariza et al., 2013). Given that α-(1–6) linkages come from the branched amylopectin molecules, a lower content of amylopectin in the starch granule leads to smaller DB values (Nilsson et al., 1996) Thus, the lower DB value presented by the *C22* variety starch can be attributed to its higher amylose content with respect to the other Arracacha starches studied.

3.4. DSC analysis

Figure 4 shows the DSC thermograms of the different yellow Arracacha starch samples; furthermore, Table 3 shows the gelatinization parameters obtained from those thermograms. All four starches had an endothermic peak corresponding to the gelatinization of the starch granule. As with other results, starches from the *Com*, *Car*, and *YH* varieties showed a similar behavior, with gelatinization temperature around 60 °C. This value agrees with previous reports for Arracacha starches (Albano et al., 2014; Castanha et al., 2018; dos Santos et al.,

Table 3. RVA and DSC parameters of the different yellow Arracacha Starches. Pasting temperature (PT), peak viscosity (PV), hot paste viscosity (HPV) at the end of the temperature plateau at 90 °C, and the cool paste viscosity (CPV) at 50 °C, breakdown (BD), setback (SB), and consistency (CS). Onset Temperature (T_0), Peak Temperature (T_p), Gelatinization Entalpy (ΔH_g).

Starch	RVA							DSC		
	PT (°C)	PV (mPa*s)	HPV (mPa*s)	CPV (mPa*s)	BD (mPa*s)	SB (mPa*s)	CS (mPa*s)	T_0 (°C)	T_p (°C)	ΔH_g (J/g)
Com	60.9 ± 0.5^a	899 ± 3^a	752 ± 2^a	856 ± 5^a	146 ± 3^a	-43 ± 1^a	104 ± 5^a	51.7 ± 0.3^a	60.7 ± 0.2^a	2.3 ± 0.1^a
Car	59.3 ± 0.2^a	841 ± 5^b	700 ± 10^b	820 ± 3^b	140 ± 4^a	-20 ± 4^b	120 ± 2^b	51.3 ± 0.2^a	60.1 ± 0.2^a	2.1 ± 0.1^a
C22	62.8 ± 0.3^b	960 ± 4^c	916 ± 3^c	1021 ±8^c	43 ± 2^b	61 ± 2^c	105 ± 3^a	54.5 ± 0.2^b	63.1 ± 0.3^b	2.1 ± 0.2^a
YH	60.6 ± 0.7^a	838 ± 1^d	743± 5^d	847 ± 3^d	65 ± 5^c	8 ± 1^d	104 ± 4^a	51.7 ± 0.1^a	60.3 ± 0.1^a	2.2 ± 0.1^a

Means with different superscripts are significantly different in their respective column ($p < 0.05$).

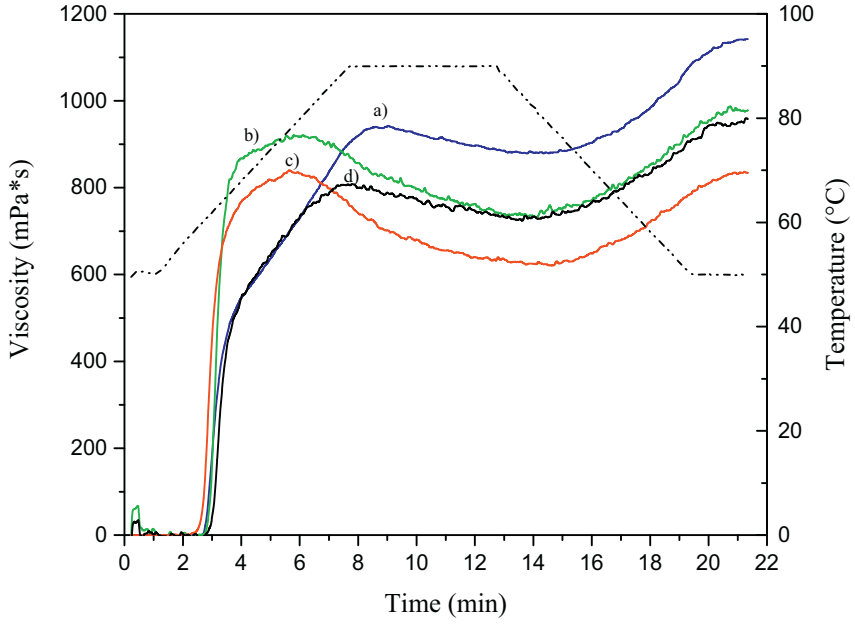

Figure 5. Pasting profiles of the four yellow Arracacha starches. a) *C22*; b) *Car*; c) *YH*; and d) *Com*.

2018; Londoño-Restrepo et al., 2018) Moreover, starch from the *C22* variety presented a slightly higher gelatinization temperature 63.1 ± 0.3 °C ($p < 0.05$), a result that can be related to its highest amylose content. Starch gelatinization is a complex process that involves steps, such as water molecules penetrating the starch granule, especially the amorphous regions, and creating disruptive forces that are transmitted into the crystalline regions, and, as such, gelatinization temperature is dependent of the granule size and amylose content (BeMiller, 2011; Ratnayake and Jackson, 2008; Wang and Copeland, 2013). Previous reports have shown that higher amylose content in rice starches lead to increasing gelatinization temperatures (Varavinit et al., 2003) This has also been reported for starches from tubers, such as cassava and yam (Charles et al., 2005; Freitas et al., 2004).

3.5. Pasting properties

The pasting properties and relative pasting curves of the four Arracacha starch samples are illustrated in Table 3 and Figure 5, respectively. All four starches had similar PT around 60 °C, with only the *C22* starch presenting a slightly higher temperature at 62 °C. The PV was also higher for the *C22* starch, reaching 960.2 cP, while the other three starches remained in the range from 800 - 900 mPa*s. The highest PV value for the *C22* starch can be explained by its higher amylose content, as it has been reported that higher amylose contents in the starch granules can lead to higher paste viscosity (Londoño-Restrepo et al., 2018; Rincón-Londoño et al., 2016; Varavinit et al., 2003). Furthermore, CPV values were also higher for the *C22* starch paste (1021.4 mPa*s) than for the other three starches (820–855 mPa*s). CPV is related to the rearrangement of the amylose molecules, mostly due to aggregation process, thus, the higher amylose content in the starch granules can lead for

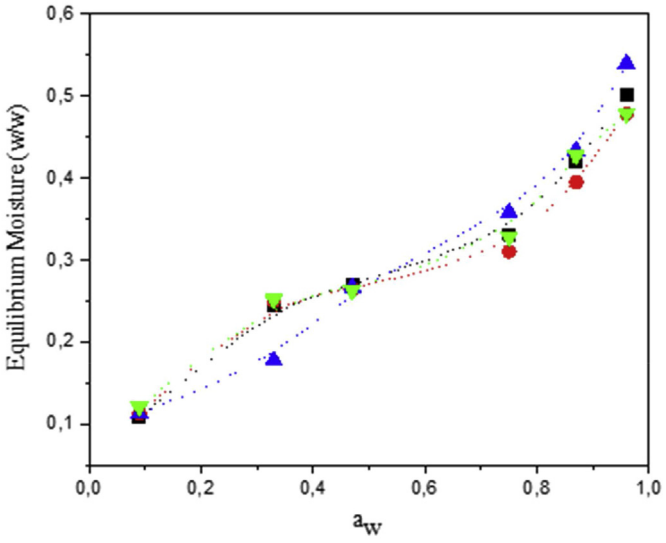

Figure 6. Sorption isotherms of the four Arracacha starches. (■) *Com*; (●) *Car*; (▲) *C22*; and (▼) *YH*. *Dotted line were drawn to guide the eye.*

Table 4. Constant parameters obtained through the mathematical fitting of the B.E.T and G.A.B models to the sorption isotherms of the different yellow Arracacha starches. T = 25 °C.

Mathematical Model	Parameter	Com	Car	C22	YH
B.E.T	W_0	0.158	0.154	0.144	0.159
	C	23.541	24.286	19.157	24.158
	R^2	0.965	0.952	0.976	0.967
G.A.B	W_0	0.217	0.208	0.180	0.204
	C	22.458	26.352	18.896	23.903
	k	0.584	0.573	0.699	0.579
	R^2	0.945	0.931	0.931	0.919

Table 5. Rapidly digested starch (RSD), slowly digested starch (SDS), and resistant starch (RS) contents of the four yellow Arracacha starches.

Starch	RDS (%)	SDS (%)	RS (%)
Com	57.1 ± 0.3^a	31.1 ± 0.2^a	10.1 ± 0.3^a
Car	63.4 ± 0.2^b	21.6 ± 0.3^b	12.9 ± 0.5^b
C22	52.7 ± 0.4^c	24.8 ± 0.3^c	15.3 ± 0.4^c
YH	61.9 ± 0.2^b	22.4 ± 0.1^b	12.1 ± 0.2^b

Means with different superscripts are significantly different in their respective column ($p < 0.05$).

higher CPV values (Arocas et al., 2009; Kong et al., 2015). Furthermore, the *C22* starch showed the highest SB and lowest BD values among the four samples. The BD measures the paste resistance to heat and shear, while SB can be used as an index of the starch retrogradation (Kong et al., 2015). Results indicate that the *C22* starch has a higher tendency to retrogradation.

3.6. Water sorption isotherms

Sorption isotherms obtained for the four Arracacha starch samples at 25 °C are presented in Figure 6. The experimental data represent the mean of three replications. All four samples showed increasing equilibrium moisture content as water activity was increased; furthermore, they presented a sigmoidal shape that is commonly assigned to Type II isotherms, according to the Brunauer's classification (Brunauer et al., 1940). Several authors have reported that sorption isotherms for different starches can be assigned to the Type II classification (Al-Muhtaseb et al., 2004; Cardoso and Pena, 2014; da Costa et al., 2013; Peng et al., 2007; Perdomo et al., 2009; Thys et al., 2010).

Table 4 shows the fitting constants of the different mathematical models studied and their correlation coefficients. All four starches showed good correlation with the two models used (B.E.T and G.A.B) and starches from the *Com*, *Car,* and *YH* varieties had similar constant values, while the *C22* differed slightly. The B.E.T and G.A.B models allow evaluating monolayer moisture content of food products (Chatakanonda et al., 2003). In both models, the *C22* starch presented lower W_0 values than the other three starches, indicating lower water molecule sorption in the monolayer. It seems that the higher amylose content of the *C22* starch affected interaction with water molecules, however, further analyses are required.

3.7. In-vitro digestibility

Finally, the amounts of RDS, SDS, and RS on the four Arracacha starch samples are presented in Table 5. All four starches had relative high RS values (>10%). These values agree with the resistance to enzymatic digestion associated with starches with B-type semi-crystalline structures (Englyst et al., 1992; Lovera et al., 2017). Among the four starches, the *C22* presented the highest content of RS (15.3 ± 0.4%). A positive relation has been reported between amylose and RS contents in the starch granule, given that higher amylose content allows stronger starch granules (reflected in their RC and gelatinization temperature values) that are more resistant to enzymatic hydrolysis (Utrilla-Coello et al., 2014; Zhu et al., 2011). Once again, the higher amylose content of the *C22* starch separates it from the other three starches, allowing for higher RS content.

4. Conclusion

Previous studies reported no significant difference among the main subdivision of the Arracacha roots (purple, yellow, and white), however, our results showed that significant differences exist among the different sub-varieties, specially, yellow variety. Starch from the *C22* sub-variety presented higher amylose content that the other three starches studied. This led to changes in other properties studied such as lower relative crystallinity, lower degree of branching, and higher gelatinization temperature and resistant starch content. Our results show that there can be significant difference among starches from different Arracacha sub-varieties, increasing the probability of finding new applications to this important Andean Tuber. This study marks an initial step in the comprehensive studied of starch from different Arracacha sub-varieties both from the yellow, and the other two types, that are commonly growth in Colombia and other Andean countries.

Declarations

Author contribution statement

Magda I. Pinzon: Conceived and designed the experiments; Performed the experiments.

Leidy T. Sanchez: Performed the experiments; Analyzed and interpreted the data.

Cristian C. Villa: Conceived and designed the experiments; Analyzed and interpreted the data; Wrote the paper.

Funding statement

This work was supported by Universidad del Quindio (Project 887).

Competing interest statement

The authors declare no conflict of interest.

Additional information

No additional information is available for this paper.

Acknowledgements

The authors want to thank Facultad de Ciencias Agropecuarias, Programa de Ingenieria de Alimentos and Programa de Quimica and AGROSAVIA for their support.

References

Acevedo-Guevara, L., Nieto-Suaza, L., Sanchez, L.T., Pinzon, M.I., Villa, C.C., 2018. Development of native and modified banana starch nanoparticles as vehicles for curcumin. Int. J. Biol. Macromol. 111, 498–504.

Al-Muhtaseb, A.H., McMinn, W.A.M., Magee, T.R.A., 2004. Water sorption isotherms of starch powders: Part 1: mathematical description of experimental data. J. Food Eng. 61 (3), 297–307.

Albano, K.M., Franco, C.M.L., Telis, V.R.N., 2014. Rheological behavior of Peruvian carrot starch gels as affected by temperature and concentration. Food Hydrocolloids 40, 30–43.

Ambardekar, A.A., Siebenmorgen, T.J., Pereira, T., 2011. Colorimetric method for rapidly predicting rice amylose content. Cereal Chem. 88 (6), 560–563.

A.O.A.C., Official Methods of Analysis, 1990. In: Association of Official Analytical Chemists, fifteen, II. The Association, Arlington, VA.

A.O.A.C., Official Methods of Analysis, 2002. In: Association of Official Analytical Chemists, seventeen, II. The Association, Arlington, VA.

Arocas, A., Sanz, T., Fiszman, S.M., 2009. Clean label starches as thickeners in white sauces. Shearing, heating and freeze/thaw stability. Food Hydrocolloids 23 (8), 2031–2037.

Atichokudom-chai, N., Shobsngob, S., Chinachoti, P., Varavinit, S., 2001. A study of some physicochemical properties of high-crystalline tapioca starch. Starch - Stärke 53 (11), 577–581.

BeMiller, J.N., 2011. Pasting, paste, and gel properties of starch–hydrocolloid combinations. Carbohydr. Polym. 86 (2), 386–423.

Brunauer, S., Deming, L.S., Deming, W.E., Teller, E., 1940. On a theory of the van der Waals adsorption of gases. J. Am. Chem. Soc. 62 (7), 1723–1732.

Cai, J., Man, J., Huang, J., Liu, Q., Wei, W., Wei, C., 2015. Relationship between structure and functional properties of normal rice starches with different amylose contents. Carbohydr. Polym. 125, 35–44.

Cardoso, J.M., Pena, R.d.S., 2014. Hygroscopic behavior of banana (Musa ssp. AAA) flour in different ripening stages. Food Bioprod. Process. 92 (1), 73–79.

Castanha, N., Villar, J., Matta Junior, M.D.d., Anjos, C.B. P.d., Augusto, P.E.D., 2018. Structure and properties of starches from Arracacha (Arracacia xanthorrhiza) roots. Int. J. Biol. Macromol. 117, 1029–1038.

Cisneros, F.H., Zevillanos, R., Cisneros-Zevallos, L., 2009. Characterization of starch from two ecotypes of Andean Achira roots (Canna edulis). J. Agric. Food Chem. 57 (16), 7363–7368.

Cortella, A.R., Pochettino, M.L., 1995. Comparative morphology of starch of three Andean tubers. Starch - Stärke 47 (12), 455–461.

Cruz, G., Ribotta, P., Ferrero, C., Iturriaga, L., 2016. Physicochemical and rheological characterization of Andean tuber starches: potato (Solanum tuberosum ssp. Andigenum), Oca (Oxalis tuberosa Molina) and Papalisa (Ullucus tuberosus Caldas). Starch - Stärke 68 (11-12), 1084–1094.

Charles, A.L., Chang, Y.H., Ko, W.C., Sriroth, K., Huang, T.C., 2005. Influence of amylopectin structure and amylose content on the gelling properties of five cultivars of cassava starches. J. Agric. Food Chem. 53 (7), 2717–2725.

Chatakanonda, P., Dickinson, L.C., Chinachoti, P., 2003. Mobility and distribution of water in cassava and potato starches by 1H and 2H NMR. J. Agric. Food Chem. 51 (25), 7445–7449.

Chávez-Salazar, A., Bello-Pérez, L.A., Agama-Acevedo, E., Castellanos-Galeano, F.J., Álvarez-Barreto, C.I., Pacheco-Vargas, G., 2017. Isolation and partial characterization of starch from banana cultivars grown in Colombia. Int. J. Biol. Macromol. 98, 240–246.

Chung, H.-J., Liu, Q., Hoover, R., 2009. Impact of annealing and heat-moisture treatment on rapidly digestible, slowly digestible and resistant starch levels in native and gelatinized corn, pea and lentil starches. Carbohydr. Polym. 75 (3), 436–447.

Chung, H.-J., Liu, Q., Lee, L., Wei, D., 2011. Relationship between the structure, physicochemical properties and in vitro digestibility of rice starches with different amylose contents. Food Hydrocolloids 25 (5), 968–975.

da Costa, F.J.O.G., Leivas, C.L., Waszczynskyj, N., Bueno de Godoi, R.C., Helm, C.V., Colman, T.A.D., Schnitzler, E., 2013. Characterisation of native starches of seeds of Araucaria angustifolia from four germplasm collections. Thermochim. Acta 565, 172–177.

Dankar, I., Haddarah, A., Omar, F.E.L., Pujolà, M., Sepulcre, F., 2018. Characterization of food additive-potato starch complexes by FTIR and X-ray diffraction. Food Chem. 260, 7–12.

dos Santos, T.P.R., Franco, C.M.L., Demiate, I.M., Li, X.-H., Garcia, E.L., Jane, J.-l., Leonel, M., 2018. Spray-drying and extrusion processes: effects on morphology and physicochemical characteristics of starches isolated from Peruvian carrot and cassava. Int. J. Biol. Macromol. 118, 1346–1353.

Englyst, H.N., Kingman, S.M., Cummings, J.H., 1992. Classification and measurement of nutritionally important starch fractions. Eur. J. Clin. Nutr. 46 (Suppl 2), S33–50. http://europepmc.org/abstract/MED/1330528.

Freitas, R.A., Paula, R.C., Feitosa, J.P.A., Rocha, S., Sierakowski, M.R., 2004. Amylose contents, rheological properties and gelatinization kinetics of yam (Dioscorea alata) and cassava (Manihot utilissima) starches. Carbohydr. Polym. 55 (1), 3–8.

Gutiérrez Malaxechebarría, Á.M., 2011. Nueva aparcería en la producción de arracacha (arracacia xanthorrhiza) en Cajamarca (Colombia). Cuad. Desarro. Rural 8, 205–228. http://www.scielo.org.co/scielo.php?script=sci_arttext&pid=S0122-14502011000200009&nrm=iso.

Kong, X., Zhu, P., Sui, Z., Bao, J., 2015. Physicochemical properties of starches from diverse rice cultivars varying in apparent amylose content and gelatinisation temperature combinations. Food Chem. 172, 433–440.

Londoño-Restrepo, S.M., Rincón-Londoño, N., Contreras-Padilla, M., Acosta-Osorio, A.A., Bello-Pérez, L.A., Lucas-Aguirre, J.C., Rodríguez-García, M.E., 2014. Physicochemical, morphological, and rheological characterization of Xanthosoma robustum Lego-like starch. Int. J. Biol. Macromol. 65, 222–228.

Londoño-Restrepo, S.M., Rincón-Londoño, N., Contreras-Padilla, M., Millan-Malo, B.M., Rodriguez-Garcia, M.E., 2018. Morphological, structural, thermal, compositional, vibrational, and pasting characterization of white, yellow, and purple Arracacha Lego-like starches and flours (Arracacia xanthorrhiza). Int. J. Biol. Macromol. 113, 1188–1197.

Lovera, M., Pérez, E., Laurentin, A., 2017. Digestibility of starches isolated from stem and root tubers of arracacha, cassava, cush–cush yam, potato and taro. Carbohydr. Polym. 176, 50–55.

Magallanes-Cruz, P.A., Flores-Silva, P.C., Bello-Perez, L.A., 2017. Starch structure influences its digestibility: a review. J. Food Sci. 82 (9), 2016–2023.

Moraes, J., Alves, F.S., Franco, C.M.L., 2013. Effect of ball milling on structural and physicochemical characteristics of cassava and Peruvian carrot starches. Starch - Stärke 65 (3-4), 200–209.

Moraes, J., Branzani, R.S., Franco, C.M.L., 2014. Behavior of Peruvian carrot (Arracacia xanthorrhiza) and cassava (Manihot esculenta) starches subjected to heat-moisture treatment. Starch - Stärke 66 (7-8), 645–654.

Nilsson, G.S., Gorton, L., Bergquist, K.-E., Nilsson, U., 1996. Determination of the degree of branching in normal and amylopectin type potato starch with 1H-NMR spectroscopy improved resolution and two-dimensional spectroscopy. Starch - Stärke 48 (10), 352–357.

Peng, G., Chen, X., Wu, W., Jiang, X., 2007. Modeling of water sorption isotherm for corn starch. J. Food Eng. 80 (2), 562–567.

Perdomo, J., Cova, A., Sandoval, A.J., García, L., Laredo, E., Müller, A.J., 2009. Glass transition temperatures and water sorption isotherms of cassava starch. Carbohydr. Polym. 76 (2), 305–313.

Pozo, C., Rodríguez-Llamazares, S., Bouza, R., Barral, L., Castaño, J., Müller, N., Restrepo, I., 2018. Study of the structural order of native starch granules using combined FTIR and XRD analysis. J. Polym. Res. 25 (12), 266.

Ratnayake, W.S., Jackson, D.S., 2008. Chapter 5 starch gelatinization. In: Advances in Food and Nutrition Research. Academic Press, pp. 221–268.

Rincón-Londoño, N., Millan-Malo, B., Rodríguez-García, M.E., 2016. Analysis of thermal pasting profile in corn starch rich in amylose and amylopectin: physicochemical transformations, part II. Int. J. Biol. Macromol. 89, 43–53.

Rocha, T.S., Cunha, V.A.G., Jane, J.-l., Franco, C.M.L., 2011. Structural characterization of Peruvian carrot (arracacia xanthorrhiza) starch and the effect of annealing on its semicrystalline structure. J. Agric. Food Chem. 59 (8), 4208–4216.

Schmitz, S., Dona, A.C., Castignolles, P., Gilbert, R.G., Gaborieau, M., 2009. Assessment of the extent of starch dissolution in dimethyl sulfoxide by 1H NMR spectroscopy. Macromol. Biosci. 9 (5), 506–514.

Sevenou, O., Hill, S.E., Farhat, I.A., Mitchell, J.R., 2002. Organisation of the external region of the starch granule as determined by infrared spectroscopy. Int. J. Biol. Macromol. 31 (1), 79–85.

Syahariza, Z.A., Sar, S., Hasjim, J., Tizzotti, M.J., Gilbert, R.G., 2013. The importance of amylose and amylopectin fine structures for starch digestibility in cooked rice grains. Food Chem. 136 (2), 742–749.

Tappiban, P., Smith, D.R., Triwitayakorn, K., Bao, J., 2019. Recent understanding of starch biosynthesis in cassava for quality improvement: a review. Trends Food Sci. Technol. 83, 167–180.

Thys, R.C.S., Noreña, C.P.Z., Marczak, L.D.F., Aires, A.G., Cladera-Olivera, F., 2010. Adsorption isotherms of pinhão (Araucaria angustifolia seeds) starch and thermodynamic analysis. J. Food Eng. 100 (3), 468–473.

Tizzotti, M.J., Sweedman, M.C., Tang, D., Schaefer, C., Gilbert, R.G., 2011. New (1)h NMR procedure for the characterization of native and modified food-grade starches. J. Agric. Food Chem. 59 (13), 6913–6919.

Utrilla-Coello, R.G., Rodríguez-Huezo, M.E., Carrillo-Navas, H., Hernández-Jaimes, C., Vernon-Carter, E.J., Alvarez-Ramirez, J., 2014. In vitro digestibility, physicochemical, thermal and rheological properties of banana starches. Carbohydr. Polym. 101, 154–162.

Varavinit, S., Shobsngob, S., Varanyanond, W., Chinachoti, P., Naivikul, O., 2003. Effect of amylose content on gelatinization, retrogradation and pasting properties of flours from different cultivars of Thai rice. Starch - Stärke 55 (9), 410–415.

Vieira, F.C., Sarmento, S.B.S., 2008. Heat-moisture treatment and enzymatic digestibility of Peruvian carrot, sweet potato and ginger starches. Starch - Stärke 60 (5), 223–232.

Villa, C.C., Sanchez, L.T., Rodriguez-Marin, N.D., 2019. Starch Nanoparticles and Nanocrystals as Bioactive Molecule Carriers, pp. 91–98.
Wang, S., Copeland, L., 2013. Molecular disassembly of starch granules during gelatinization and its effect on starch digestibility: a review. Food Function 4 (11), 1564–1580.
Wang, S., Li, C., Copeland, L., Niu, Q., Wang, S., 2015. Starch retrogradation: a comprehensive review. Compr. Rev. Food Sci. Food Saf. 14 (5), 568–585.
Yong, H., Wang, X., Sun, J., Fang, Y., Liu, J., Jin, C., 2018. Comparison of the structural characterization and physicochemical properties of starches from seven purple sweet potato varieties cultivated in China. Int. J. Biol. Macromol. 120, 1632–1638.
Zeng, F., Gao, Q.-y., Han, Z., Zeng, X.-a., Yu, S.-j., 2016. Structural properties and digestibility of pulsed electric field treated waxy rice starch. Food Chem. 194, 1313–1319.
Zhang, L., Zhao, L., Bian, X., Guo, K., Zhou, L., Wei, C., 2018. Characterization and comparative study of starches from seven purple sweet potatoes. Food Hydrocolloids 80, 168–176.
Zhu, L.-J., Liu, Q.-Q., Wilson, J.D., Gu, M.-H., Shi, Y.-C., 2011. Digestibility and physicochemical properties of rice (Oryza sativa L.) flours and starches differing in amylose content. Carbohydr. Polym. 86 (4), 1751–1759.